Tracking Phospholipid Populations in Polymorphism by Sideband Analyses of ^{31}P Magic Angle Spinning NMR

Liam Moran and Nathan Janes
Department of Pathology, Anatomy, and Cell Biology, Medical College of Thomas Jefferson University, Philadelphia, Pennsylvania 19107 USA

ABSTRACT A method was developed to track the distributional preferences of phospholipids in polymorphism based on sideband analyses of the ^{31}P magic angle spinning nuclear magnetic resonance spectra. The method was applied to lipid mixtures containing phosphatidylcholine (PtdCho), phosphatidylethanolamine (PtdEtn) and either cholesterol (Chol) or tetradecane, as well as mixtures containing the anionic phosphatidylmethanol, phosphatidylethanolamine, and diolein. The phospholipid composition of coexisting lamellar (L_α) and inverted hexagonal (H_{II}) phases remained constant throughout the $L_\alpha \rightarrow H_{II}$ transition in all mixtures, except those that contained saturated PtdCho and unsaturated PtdEtn in the presence of cholesterol—mixtures that are known to be microimmiscible because of favored associations between Chol and saturated acyl chains. In the latter mixture, saturated PtdCho was enriched in the planar bilayer structure, and unsaturated PtdEtn was enriched in the highly curved H_{II} structure. This enrichment was coincident with an increase in the transition width. When compositional heterogeneity among coexisting phases was observed, it appeared that preexisting lateral microheterogeneities led to compositionally distinct transitional clusters, such that the distributional preferences that resulted were not those of the individual phospholipids.

INTRODUCTION

Packing mismatches in membranes create a curvature stress that has been implicated as a determinant of membrane structure, protein function, and fusion (de Kruijff et al., 1985; de Kruijff, 1997; Epand, 1996, 1997; Hui and Sen, 1989; Israelachvili et al., 1980). One approach to the quantitation of the curvature stress imparted by individual membrane constituents upon the planar bilayer structure is to correlate the effects of dilute levels of that constituent upon the equilibrium midpoint temperature (T_H) of a matrix that undergoes a transition between a planar bilayer structure (L_α) and a highly curved inverted hexagonal (H_{II}) structure (Hornby and Cullis, 1981; Epand, 1985; Lee et al., 1993, 1996; Janes, 1996). Constituents that relieve the curvature stress present in the bilayer act to stabilize the bilayer and raise T_H. The converse holds for agents that increase the curvature stress. The constituent's curvature energy in the bilayer matrix is the product of the change in T_H and the transition entropy (Lee et al., 1996; Janes, 1996). Implicit to the approach is that changes in T_H stem from changes in curvature stress and not from changes in the entropy of mixing due to compositional heterogeneity during the $L_\alpha \rightarrow H_{II}$ transition. Yet it may seem counterintuitive that a membrane constituent that exhibits a pronounced preference for adopting a particular phase in isolation and promotes the formation of a particular phase in a mixture would nonetheless exhibit little distributional preference for that phase throughout the phase coexistence region of an equilibrium. The inquiries that have addressed this issue have yielded mixed results (Boni and Hui, 1983; de Kruijff et al., 1979; Eriksson et al., 1985; Fenske and Cullis, 1992; Lee et al., 1996; Rand et al., 1990; Tate and Gruner, 1987; Tilcock et al., 1982).

In this article, we have demonstrated a ^{31}P magic angle spinning nuclear magnetic resonance (MAS NMR) approach to monitoring the phospholipid populations of coexisting phases throughout the $L_\alpha \rightarrow H_{II}$ (and isotropic phase, I) transition. Phospholipids in these phases have distinctive chemical shielding anisotropies (CSAs) due to the different axes of rapid motion characteristic of each phase. Individual phospholipids were resolved based on their characteristic isotropic chemical shifts. The ^{31}P spinning sideband profiles reflected the phospholipid populations in each phase.

This NMR method was applied to several lipid mixtures. Initially, a dioleoyl phosphatidylcholine (Ole_2PtdCho), dioleoyl phosphatidylethanolamine (Ole_2PtdEtn), cholesterol (Chol) mixture was examined. Previously, this mixture was reported to exhibit no qualitative differences in the phospholipid composition of coexisting phases based on wideline ^{2}H NMR (Tilcock et al., 1982) and ^{31}P NMR of aligned systems (Fenske and Cullis, 1992). Second, systems that included saturated PtdCho, Ole_2PtdEtn, and Chol were examined. Chol is known to favor interactions with saturated over unsaturated acyl chains, and to induce a fluid phase microimmiscibility that we reasoned might be expressed through the distributions of the phospholipids among coexisting phases (Kusumi et al., 1986; Pasenkiewicz-Gierula et al., 1990; Shin and Freed, 1989a,b; Shin et al., 1990, 1993; Subczynski et al., 1990). Third, a related homologous dioleoyl mixture—lacking cholesterol, but containing low levels of tetradecane—that was reported to exhibit significant

Received for publication 7 January 1998 and in final form 24 April 1998.
Address reprint requests to Dr. Nathan Janes, Department of Pathology, Anatomy, and Cell Biology, Medical College of Thomas Jefferson University, 271 Jeff Hall, 1020 Locust St., Philadelphia, Pennsylvania 19107. Tel.: 215-503-1174; Fax: 215-923-2218; E-mail: janesn@jeflin.tju.edu.

0006-3495/98/08/867/13 $2.00

distributional preferences based on indirect evidence was examined (Rand et al., 1990). Fourth, a system containing an anionic phospholipid (phosphatidylmethanol, PtdMe), PtdEtn, and low levels of diolein was examined. This system provided a means of examining the effects of surface charge on phospholipid distribution and was relevant to our interest in the phosphatidylalkanols (Lee et al., 1993, 1996; Janes, 1996). In particular, we asked whether the distributional preferences of membrane constituents are expressed in polymorphic equilibria, whether compositional heterogeneities occur during polymorphic equilibria, and if so, what factors may be responsible for their occurrence.

MATERIALS AND METHODS

Liposome preparations

Lipids (Avanti Polar Lipids, Alabaster, AL) were assayed for purity (>99%) by thin-layer chromatography. Lipid concentrations were obtained gravimetrically. Cholesterol was obtained from Sigma (St. Louis, MO) and recrystallized three times from methanol. Tetradecane (Fisher Scientific, Pittsburgh, PA) was used without further purification. All other chemicals were obtained from Sigma.

Lipids (~60 mg) in $CHCl_3$ were dried to a thin film under a stream of dry N_2 and evacuated overnight (<10 mTorr). Liposomes were formed by vigorous vortexing after the addition of 1.5 ml of buffer solution (150 mM KCl, 10 mM Tris, 0.2 mM EGTA, pH 7.2). Two micromoles of phosphocreatine was included as a chemical shift reference. The suspension was vortexed for 5 min, allowed to stand for 30–60 min, and vortexed for an additional 5 min. The lipids were pelleted by low-speed centrifugation, and the pellet was transferred to MAS sample rotors (~130 μl).

The following samples were examined. Those containing PtdCho, Ole_2PtdEtn, and Chol had the following compositions in mole percent (mol%) ([100 $N_i/\Sigma N_i$] or mole fraction times 100): 1) Ole_2PtdCho (25), Ole_2PtdEtn (30), and Chol (45); 2) Myr_2PtdCho (21), Ole_2PtdEtn (34), and Chol (45); 3) Lau_2PtdCho (21), Ole_2PtdEtn (34), and Chol (45); 4) Myr_2PtdCho (20), Ole_2PtdEtn (80), and Chol (0); 5) Ole_2PtdCho (21), Myr_2PtdEtn (21), Ole_2PtdEtn (13), and Chol (45). Samples containing Ole_2PtdCho, Ole_2PtdEtn, and tetradecane (0.0, 1.15, 1.3, 3.1, 10 wt%) were prepared with a PtdCho/PtdEtn molar ratio of 1:3. Tetradecane (td) was not added to the lipids in chloroform because of its volatility during evacuation. Its low aqueous solubility made addition to the aqueous dispersion impractical. Consequently, neat td was added volumetrically to the dried lipid film and allowed to equilibrate with the film for 30 min before hydration. Samples containing Pam_2PtdMe, PamOlePtdEtn, and diolein were prepared with the following composition (in mol%): 1) Pam_2PtdMe (10), PamOlePtdEtn (85), and diolein (5); 2) Pam_2PtdMe (20), PamOlePtdEtn (75), and diolein (5).

^{31}P NMR

^{31}P NMR spectra were recorded on a 8.5-T solenoid interfaced with a Bruker AM spectrometer operating at 145.8 MHz and equipped with a multinuclear 5-mm MAS sample spinning probe (Doty Scientific, Columbia, SC). The static spectra were recorded with 6-μs $\pi/2$ pulses, inverse gated noise decoupling (21 kHz proton field), 22-μs preacquisition delay, 4-s recycle delay, 25 kHz spectral window, 2K points zero-filled to 4K, and ~1000 transients. Bloch decays of the MAS spectra were recorded with 1400 ± 4 Hz sample rotation, 30-μs preacquisition delays, without proton decoupling, 2-s recycle delays, a 25-kHz spectral window, 4K points zero-filled to 8K, and between 1,400 and 12,000 transients. The number of transients collected in the MAS experiments was chosen to maintain comparable signal-to-noise ratios in the sideband from the bilayer phase (second sideband to the left of the centerband). Saturation factors were obtained at selected temperatures for all phase combinations in each sample and were equal for all phospholipids. Samples were equilibrated for ≥15 min at each temperature. Except where noted, spectra represent equilibrium conditions as established by duplicate scans in the region of phase coexistence. All experiments were heating scans. The temperature was regulated to ±1°C. Chemical shifts were referenced to the isotropic PtdCho resonance, using phosphocreatine as an internal standard (−2.2 ppm).

The sideband profiles of the L_α, H_{II}, and I phases were considered to be characteristic of those structures, and changes in the sideband profiles were ascribed to changes in their relative proportions (see Results). The sideband profiles of the L_α and H_{II} phases exhibited a weak dependence on temperature and composition. Changes in the sideband profile due to these factors were more than an order of magnitude smaller than the changes in the sideband profile characteristic of the structural interchange.

MAS spectra were simulated with the program ANTIOPE (de Bouregas and Waugh, 1992). The computed transients of 201 orientations were summed. An exponential filter corresponding to the experimental linewidth was applied before the apodized transients were Fourier transformed. Spectral deconvolutions were performed with Grams/386 spectral analysis software (Galactic Industries, Salem, NH).

RESULTS

MAS NMR determination of the phospholipid populations in polymorphism

Rapid sample rotation has been used widely to increase the spectral resolution and motionally narrow the broad resonance characteristic of solids and semisolids (e.g., Woyciesjes et al., 1985; Timken et al., 1986). The analytical approach to tracking phospholipid populations in polymorphism relies on two factors illustrated in Fig. 1: 1) The phases have considerably different CSAs that vary little throughout the transition, so that the observed sideband intensities are a linear combination of sideband intensities characteristic of each phase. 2) The isotropic chemical shifts of the phospholipids are distinct.

Phospholipids arranged in a fluid bilayer yield a characteristic wideline ^{31}P NMR powder pattern (Seelig and Seelig, 1980), as shown in Fig. 1 *A* for a mixture of PtdEtn, PtdCho, and cholesterol (30:25:45 mol%) at 22°C. Phospholipids arranged in the highly curved inverted hexagonal (H_{II}) phase experience an additional axis of motion that yields the powder pattern shown in Fig. 1 *B* for the same mixture at 67°C. A narrow isotropic (I) resonance of low intensity at 0 ppm is superimposed on the latter. Isotropic resonances reflect rapid isotropic motion and are generally characteristic of highly curved cubic structures (Shyamsunder et al., 1988).

The corresponding high-resolution MAS-NMR spectra are shown in Fig. 1, *C* and *D*. Rapid rotation at the magic angle causes narrow liquid-like spectra. Slower rotation, such as that shown (1.4 kHz), creates a comb of spinning sidebands (SSBs) around the centerband (the largest peak in the spectra shown) spaced at the rotation frequency that roughly maps out the static spectrum. There are two centerbands with associated sidebands; those associated with PtdCho are 0.62 ppm upfield of PtdEtn. An additional peak, barely visible at −2.2 ppm, is from the chemical shift reference, phosphocreatine.

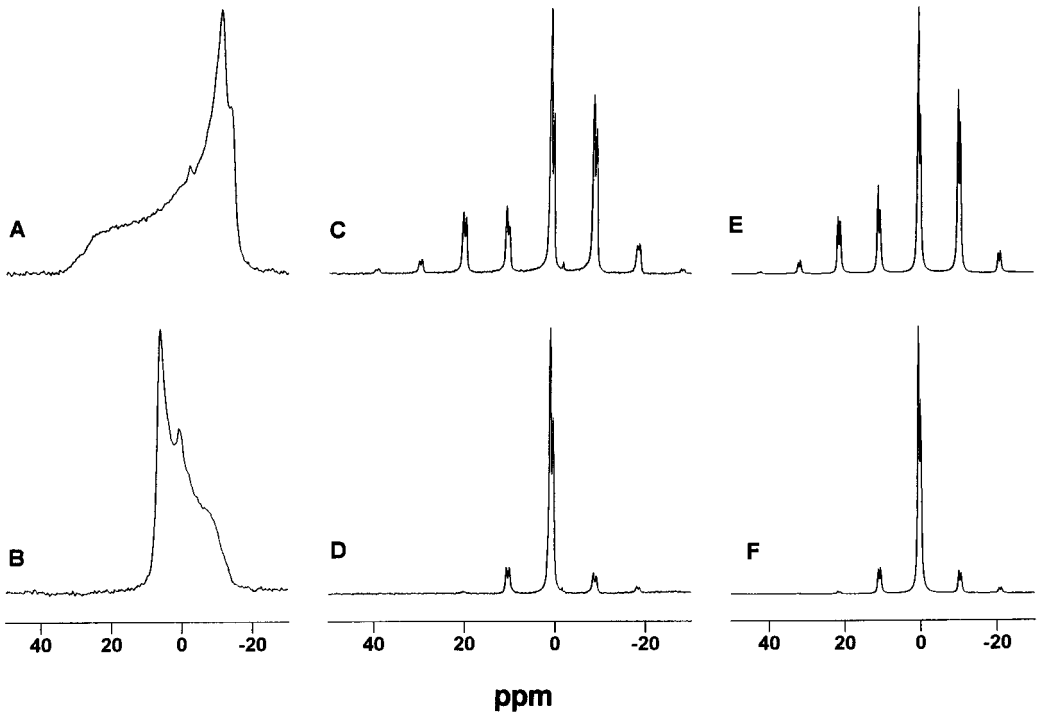

FIGURE 1 ^{31}P NMR approach to tracking phospholipid populations in polymorphism. The bilayer and inverted hexagonal structures are distinguished with ^{31}P MAS NMR. Spectra are shown for Ole_2PtdCho/Ole_2PtdEtn/Chol (25:30:45 mol%). (*A*) Nonspinning spectrum of a bilayer structure at 22°C. (*B*) Nonspinning spectrum of the inverted hexagonal structure formed in the same sample at 67°C. (*C*) MAS spectrum (1400 Hz) of *A*. (*D*) MAS (1400 Hz) spectrum of *B*. (*E*) Simulation of *C*. (*F*) Simulation of *D*. The small peak at −2.2 ppm visible in *A*, *C*, and *D* is the internal chemical shift reference standard (phosphocreatine). The isotropic peak in *B* at ~0.0 ppm is from isotropic (e.g., cubic) structures.

Shown in Fig. 1, *E* and *F*, are the ANTIOPE (de Bouregas and Waugh, 1992) simulations of the corresponding MAS spectra in Fig. 1, *C* and *D*. The CSA tensor elements were adjusted to obtain the best fit of the experimental spectra. The fitted motionally averaged chemical shielding tensor elements used in the simulation shown in Fig. 1 *E* referenced to the isotropic PtdCho peak (phosphocreatine = −2.2 ppm) were as follows: PtdEtn (24.3, −12.7, −9.7 ppm), PtdCho (27.9, −16.6, −11.3 ppm). The parameters used in Fig. 1 *F* for the inverted hexagonal phase spectra were as follows: PtdEtn (−10.2, 6.8, 5.3 ppm), PtdCho (−12.7, 6.8, 5.8 ppm). A slight deviation from axial symmetry provided best fits to the sideband patterns. Small differences between the experimental and fitted profiles may reflect incomplete averaging due to slower motions near the spinning frequency.

In the phase coexistence region of the $L_\alpha \rightarrow H_{II}$ transition, the sideband pattern obtained is a population-weighted average of the characteristic L_α and H_{II} (and I) sideband patterns. Phospholipid populations in the L_α, H_{II}, and I states were determined by monitoring changes in the sideband intensities throughout the transition. The spinning speed (1.4 kHz at 8.5 T) was chosen to provide four sidebands of significant intensity for quantitation. It was desirable that one sideband (here it was the second sideband to the left of the centerband) represent the composition of the L_α structure for facile estimation of the bilayer composition and as a presentational tool. In addition, the spinning speed chosen was sufficient to decouple ^{31}P from ^{1}H and obviate any concerns about heating due to ^{1}H irradiation.

For each phospholipid, the *i*th sideband area A^i was a linear combination of the normalized areas A^i_n characteristic for each of the *n* phases weighted by the phospholipid populations *P* in the *n*th phase:

$$A^i = \sum P_n A^i_n \qquad (1)$$

The intensities of the second left, first left, centerband, and first right sidebands were used to compute the phospholipid populations in each of the three phases. This approach led to an overdetermined system (four SSBs, three phases of unknown phospholipid populations). Populations were obtained by varying P_n to minimize the sum of the squared residuals between all four experimental sideband intensities and those computed with Eq. 1.

The analysis considered the sideband profile to be characteristic of a particular phase as determined by an initial L_α spectra or a final H_{II} spectra. When isotropic phases contributed to the endpoints, the pure reference profile is obtained by subtracting the isotropic phase deduced from the static spectrum from the centerband. From a qualitative standpoint, the second left sideband reflected the bilayer composition. The first left sideband exhibited little change for variances in the L_α/H_{II} ratio, but lost intensity with

increases in I. The centerband and first right sideband were sensitive to the compositions of all three structures.

Phospholipid distributions in Ole_2PtdCho/Ole_2PtdEtn/Chol polymorphism

^{31}P NMR spectra of the $L_\alpha \rightarrow H_{II}$ transition of a mixture of 25 mol% dioleoylphosphatidylcholine (Ole_2PtdCho), 30 mol% dioleoylphosphatidylethanolamine (Ole_2PtdEtn), and 45 mol% cholesterol (Chol) are shown at representative temperatures in Fig. 2. The static wideline and MAS spectra are shown in Fig. 2, *A* and *B*, respectively. For demonstrational purposes, the second left MAS sideband is asterisked in Fig. 2 *B*, and expansions are displayed in Fig. 2 *C*. This sideband is derived almost exclusively from the L_α structure. Its PtdCho/PtdEtn peak ratio provided a facile visual index for changes in the phospholipid composition. Slight increases in the MAS linewidths were observed during the transition (possibly because of changes in sample packing or changes in diamagnetic susceptibility that arose from the presence of the H_{II} aggregates). The PtdCho/PtdEtn intensity ratios shown in Fig. 2 *C* revealed little variation in the phospholipid composition of the bilayer throughout the transition and provided an indication that the compositions of coexisting phases were unchanged throughout the transition.

Phospholipid distributions in saturated PtdCho/Ole_2PtdEtn/Chol polymorphism

Substitution of dimyristoyl (Myr_2) PtdCho for the Ole_2PtdCho used in the previous experiment and minor adjustment of the ratios so that the equilibrium occurred at suitable temperatures (Myr_2PtdCho/Ole_2PtdEtn/Chol, 21:34:45) yielded the spectra shown at representative temperatures in Fig. 3. The static spectra shown in Fig. 3 *A* evidenced an elevation in the transition midpoint temperature from that observed for the Ole_2PtdCho series (Fig. 2). The presence of saturated chains acted to stabilize the bilayer structure. The MAS spectra are shown in Fig. 3 *B*. The asterisked sideband is expanded in Fig. 3 *C*. The phospholipid content of the bilayer became progressively enriched in PtdCho and depleted of PtdEtn, as evidenced by the change in the sideband ratio. Deconvolutions of the asterisked second left sideband pair are shown in Fig. 4 for the 28°C and 68°C points and further evidenced the 35% increase in the PtdCho/PtdEtn ratio in the bilayer. Similar deconvolutions were performed for all pairs of the four major sidebands throughout the transition for the plots shown below.

Similar experiments performed with a dilauroyl (Lau_2) PtdCho/Ole_2PtdEtn/Chol (21:34:45 mol%) mixture (sum-

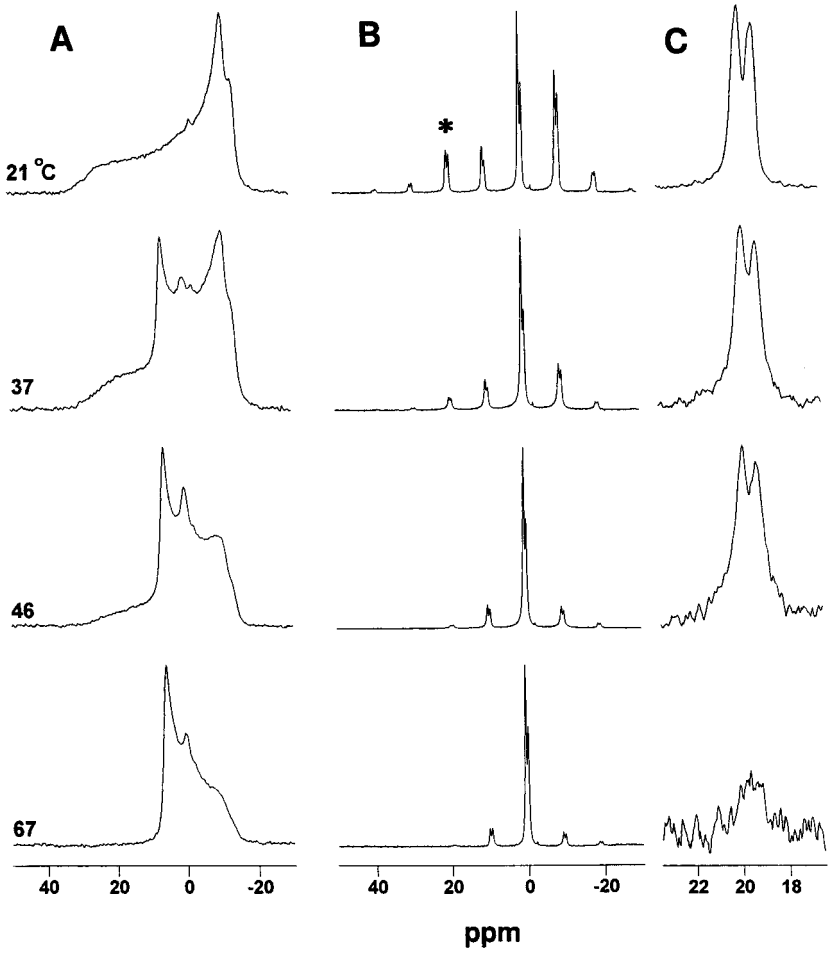

FIGURE 2 Tracking phospholipid populations in the $L_\alpha \rightarrow H_{II}$ equilibrium of Ole_2PtdCho-Ole_2PtdEtn-Chol (25:30:45 mol%). Representative spectra are shown at the temperatures indicated. (*A*) Nonspinning spectra. (*B*) MAS spectra (1400 Hz). PtdCho is shifted upfield or to lower frequencies. (*C*) Expansion of the asterisked second left spinning sideband. The vertical scale is magnified from top to bottom by 1, 3.3, 11.5, and 11.5, respectively.

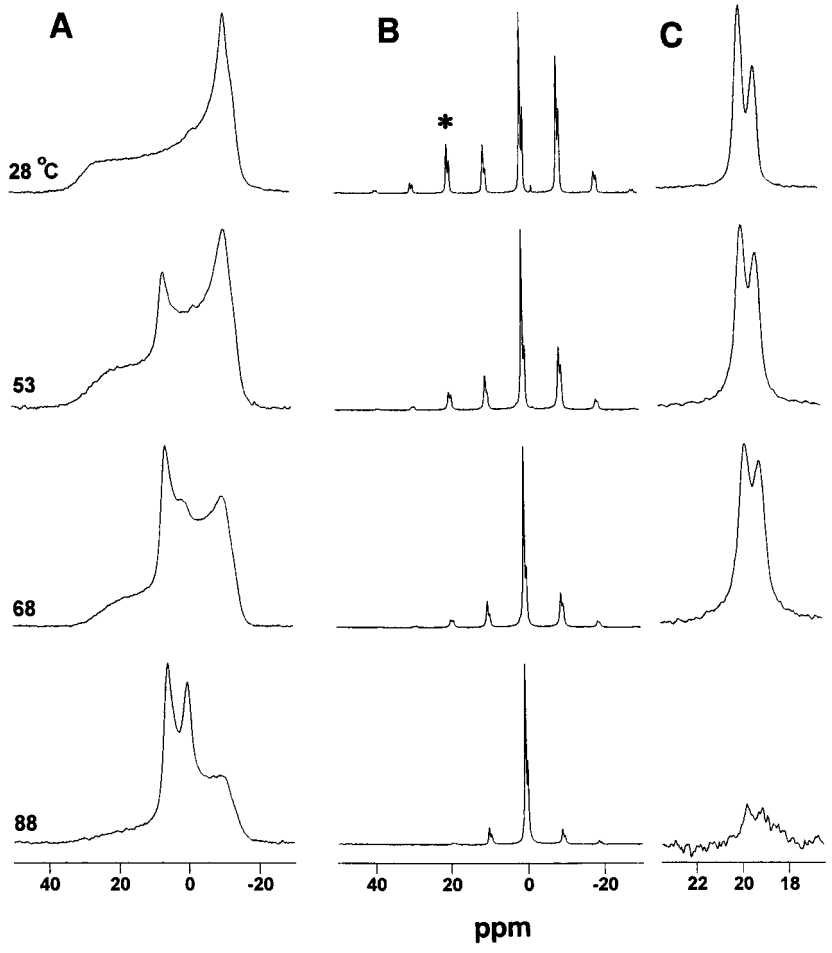

FIGURE 3 Tracking phospholipid populations in the $L_\alpha \rightarrow H_{II}$ equilibrium of Myr_2PtdCho-Ole_2PtdEtn-Chol (21:34:45 mol%). Representative spectra are shown at the temperatures indicated. (*A*) Nonspinning spectra. (*B*) MAS spectra (1400 Hz). (*C*) Expansion of the asterisked second left spinning sideband. The vertical scale is magnified from top to bottom by 1, 2.7, 6.3, and 6.3, respectively.

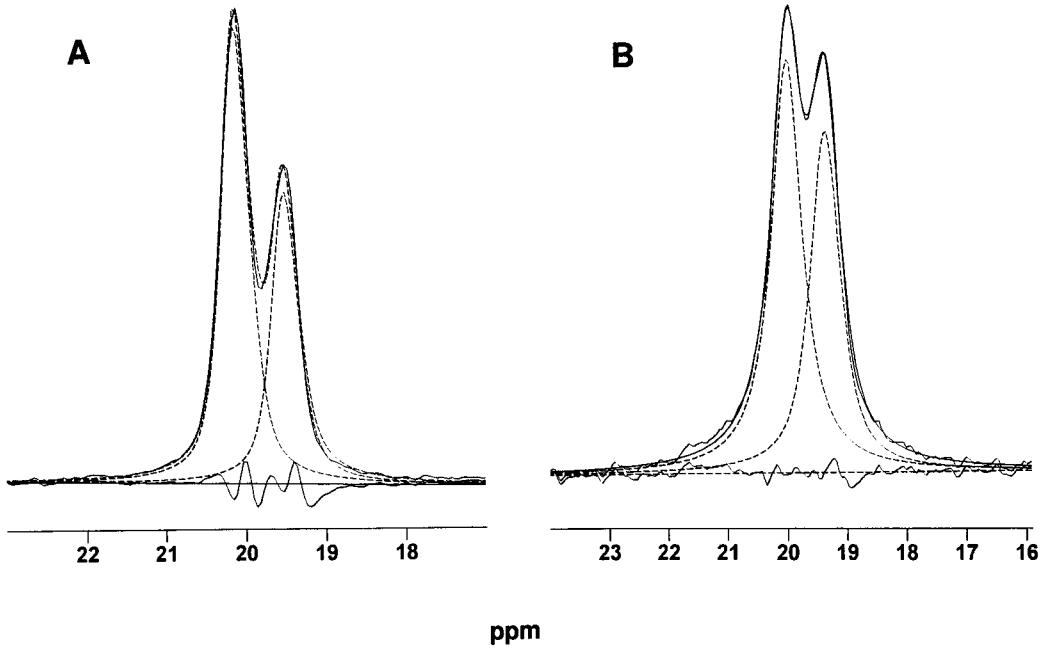

FIGURE 4 Deconvolution of the second left sideband peak pair demonstrates the changes in the PtdCho/PtdEtn population ratio that reflect changes in the phospholipid composition of the bilayer. Peaks from Fig. 3 *C* at (*A*) 28°C and (*B*) 68°C are shown (*solid lines*). The fitted spectral components and their sum are shown as dotted lines. The residuals are shown below.

marized below) also revealed an increase in the PtdCho/PtdEtn population ratio in the bilayer structure that was intermediate between that observed for the mixtures containing Ole_2PtdCho and Myr_2PtdCho. Shape theories alone would have predicted effects more extreme than those observed for Myr_2PtdCho (see the Discussion).

To address the role of cholesterol, a mixture of Myr_2PtdCho and Ole_2PtdEtn (1:4) that lacked cholesterol was examined. No changes in the PtdCho/PtdEtn ratios were detected in the absence of cholesterol (T_H = 74.9°C, transition width [75% $L_\alpha \rightarrow$ 25% L_α] = 12.4°C; see below). To address the role of nonideal mixing, a lipid mixture that was homologous to the mixture shown in Fig. 3 was examined. That is, the composite headgroup composition and the composite acyl composition were maintained. This was achieved by swapping the dimyristoyl chains of PtdCho with some of the dioleoyl chains of PtdEtn so that the mixture from Fig. 3 (Myr_2PtdCho/Ole_2PtdEtn/Chol, 21:34:45) yielded an Ole_2PtdCho/Myr_2PtdEtn/Ole_2PtdEtn/Chol (21:21:13:45) mixture. This swap transformed the disaturate from a strong promoter of the bilayer structure (Myr_2PtdCho) to a weak promoter of the H_{II} structure (Myr_2PtdEtn) without altering the cumulative membrane "shape." If mixing were ideal, the same cumulative membrane "shapes" should have yielded a similar midpoint temperature. This was not observed. The phospholipid midpoint temperature was elevated by 7.7°C (T_H = 73.1°C), and the apparent transition width was reduced ([75% $L_\alpha \rightarrow$ 25% L_α] = 7.5°C). Although the PtdEtn population now represented a sum of two species, no changes in the PtdCho/PtdEtn ratio were detected.

Summary of phospholipid distributions in PtdCho/PtdEtn/Chol

The phospholipid compositions of structures throughout the $L_\alpha \rightarrow H_{II}$ transition are summarized for all three PtdCho/Ole_2PtdEtn/Chol mixtures in Fig. 5. These data were obtained from a deconvolution of the four major sidebands as described above. Fig. 5, *A–C*, represents the dioleoyl, dilauroyl, and dimyristoyl PtdCho mixtures, respectively. The three curves in the top panels represent the fractional distribution of the total PtdCho population throughout the bilayer, inverted hexagonal, and isotropic phases. The middle panels show the same data for PtdEtn. The lower panels show the absolute population (not fractional) ratio of PtdCho/PtdEtn in the bilayer. In the Ole_2PtdCho system shown in Fig. 5 *A*, there was no significant change in the PtdCho/PtdEtn levels in the bilayer, and the apparent midpoint temperatures of PtdCho and PtdEtn were similar. In the systems where the population differences were manifest, shown in Fig. 5, *B* and *C*, the apparent midpoint temperatures for the two phospholipids diverged. The apparent

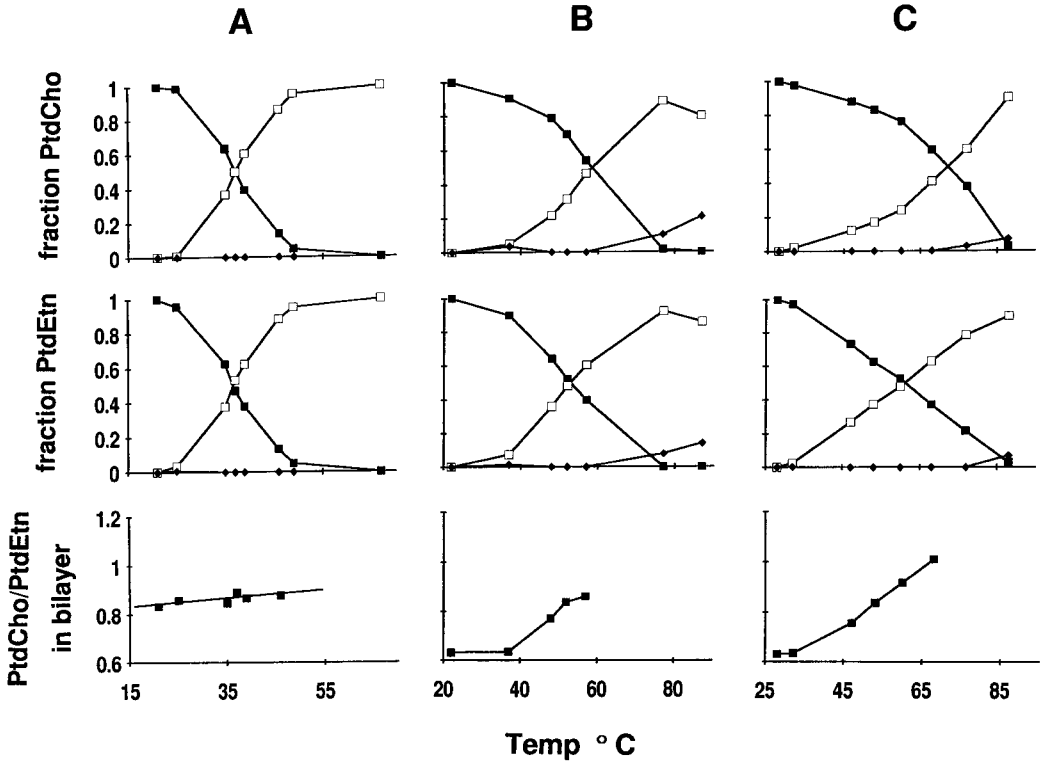

FIGURE 5 Distributional preferences of phospholipids in PtdCho/Ole_2PtdEtn/Chol polymorphism. The top and middle rows of panels depict the fraction of PtdCho and PtdEtn, respectively, in the bilayer (■), inverted hexagonal (□), and isotropic (◆) phases. The bottom row of panels represents the ratio of PtdCho/PtdEtn in the bilayer. The three lipid mixtures are as follows: (*A*) Ole_2PtdCho/Ole_2PtdEtn/Chol (25:30:45 mol%), (*B*) Lau_2PtdCho/Ole_2PtdEtn/Chol (21:34:45 mol%), (*C*) Myr_2PtdCho/Ole_2PtdEtn/Chol (21:34:45 mol%).

midpoint temperatures of the PtdCho and PtdEtn components, expressed as the temperature at which half of the phospholipid is in the planar bilayer and half is in the curved nonbilayer structures (H_{II} or I), were as follows: Ole_2PtdCho system, PtdCho 37.0°C, PtdEtn 36.5°C; Lau_2PtdCho system, PtdCho 58.5°C, PtdEtn 52.5°C; Myr_2PtdCho system, PtdCho 71.8°C, PtdEtn 61.5°C.

To better illustrate the polymorphic tendencies of the phospholipids throughout the transition, the individual phospholipid populations were summed for each phase and plotted in Fig. 6. This presentation revealed substantial differences in the apparent width of the transition for these three lipid mixtures that coincided with the compositional changes evidenced by the PtdCho/PtdEtn ratios. To quantitate the phospholipid phase distributions, an apparent mole fraction partition coefficient K_p^{app} was calculated as follows:

$$K_p^{app} = \frac{\text{mol PtdCho } (L_\alpha)/[\text{mol PtdCho } (L_\alpha) + \text{mol PtdEtn } (L_\alpha)]}{\text{mol PtdCho } (H_{II})/[\text{mol PtdCho } (H_{II}) + \text{mol PtdEtn } (H_{II})]} \quad (2)$$

This quantity resembled the traditional partition coefficient in mole fraction units, except that it focused on the phospholipids and neglected cholesterol. (Inherent within the partition coefficient formalism is the assumption of a true equilibrium distribution. This is not the case here. See the Discussion.) The values of K_p^{app} at the apparent midpoint of the bilayer to nonbilayer transition for the Ole_2PtdCho, Lau_2PtdCho, Myr_2PtdCho mixtures were 1.04, 1.53, and 1.91, respectively. The apparent transition width based on the phospholipid phase behavior, defined as the heating degrees necessary to alter the equilibrium from 75% $L_\alpha \rightarrow$ 25% L_α, is plotted against the apparent partition coefficient in Fig. 7. The excellence of the correlation and its seeming linearity almost certainly overstated the actual situation, given the neglect of cholesterol and the slightly different PtdCho/PtdEtn ratios employed. Nonetheless, the correlation clearly evidenced the expected linkage between width and composition.

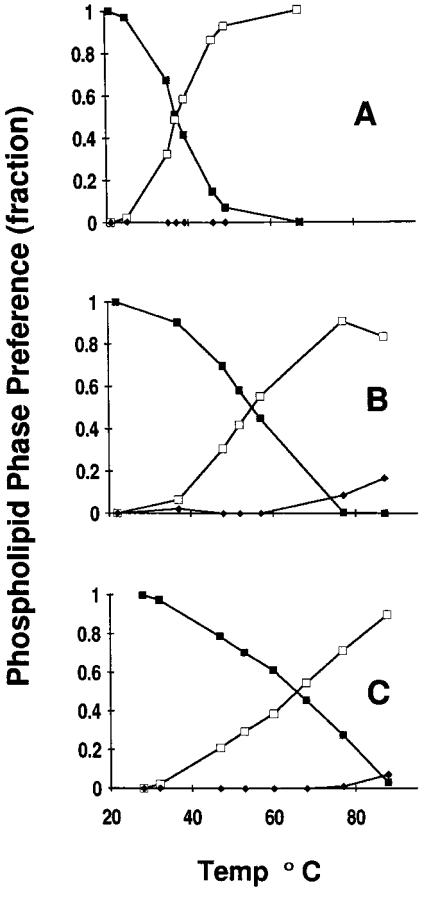

FIGURE 6 Phospholipid populations in polymorphism. The individual phospholipid phase preferences shown in Fig. 5 are summed and presented as a function of temperature. *A, B, C* and the symbols are defined in Fig. 5.

Effects of tetradecane on phospholipid distributions in Ole_2PtdCho/Ole_2PtdEtn

^{31}P NMR spectra of an Ole_2PtdCho/Ole_2PtdEtn mixture (1:3 mole ratio) in the absence and presence of 1.3 wt% tetradecane (td) at 22°C after 5 h of equilibration are shown in Fig. 8. The phospholipid composition of the bilayer remained constant throughout the td-induced transition, as evidenced by the expansion of the second left sideband. The results are summarized in Table 1 for a wider range of td concentrations. Equilibration times for experiments with td were long and somewhat variable. To hasten equilibration, td was allowed to equilibrate with the dried lipid film for 30 min. Except where indicated, Table 1 is based on spectra obtained 1–2 h after hydration and does not necessarily represent equilibrium values. No evidence that td induced any changes in the PtdCho/PtdEtn ratio was observed. The transition was also monitored as a function of temperature in the absence of td, and no changes in the PtdCho/PtdEtn ratios were apparent.

Distribution of an anionic phospholipid (PtdMe-PamOlePtdEtn-diolein)

The phosphatidylalkanols possess hydrophobic alkyl headgroups that give rise to unusual properties (Lee et al., 1996;

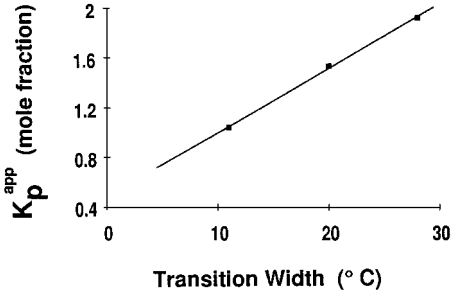

FIGURE 7 Correlation between the distributional preferences of the phospholipids and the transition width. The apparent partition coefficient of phosphatidylcholine (see text) is plotted against the apparent width of the transition and fit to an empirical linear function.

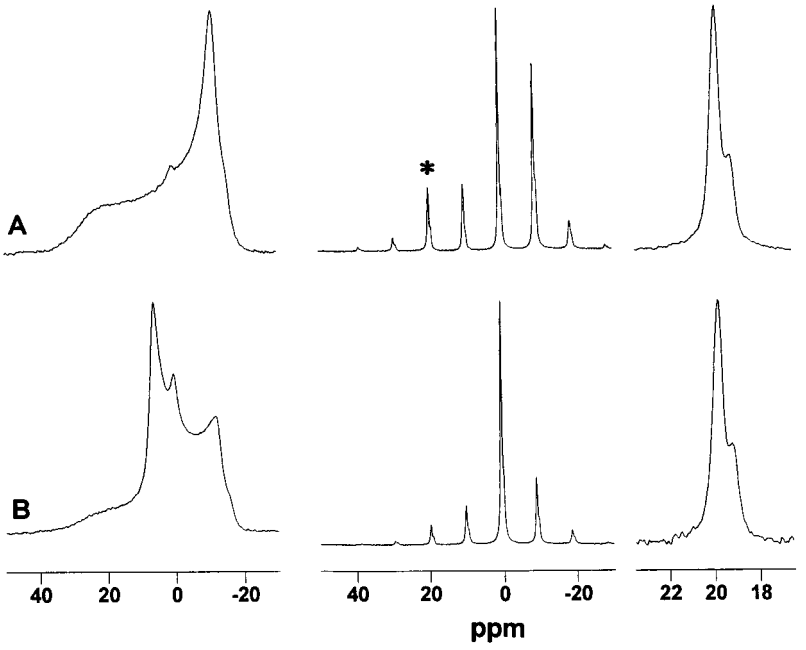

FIGURE 8 Effects of tetradecane on the distributional preferences of $Ole_2PtdCho/Ole_2PtdEtn$ (1:3) polymorphism. ^{31}P NMR spectra (*A*) in the absence and (*B*) in the presence of 1.3 wt% tetradecane at 22°C after 5 h equilibration. (Left) Static, (middle) MAS (1.4 kHz), and (right) expansion of the asterisked second sideband, respectively.

Victorov et al., 1994). Fig. 9 contains ^{31}P NMR spectra for a dipalmitoyl phosphatidylmethanol (Pam_2PtdMe), 1-palmitoyl-2-oleoyl-phosphatidylethanolamine (PamOlePtdEtn), and diolein (20:75:5 mol%) sample at representative temperatures. The chemical shift anisotropy of PtdMe gave rise to a distinct asymmetry (perpendicular edge) in the static spectrum downfield from that of PtdEtn. The centerbands and sidebands associated with PtdMe were 1.1 ppm downfield of the $Ole_2PtdEtn$ signal. The increased resolution allowed quantitative inquiries at modest PtdMe levels. This transition proceeded to the isotropic phase with low levels of H_{II} formed. The constancy of the PtdMe/PtdEtn ratio was demonstrated by the second left sideband region shown in Fig. 9 *C*, which indicated that the bilayer did not become significantly enriched in either phospholipid. PtdMe-PamOle-PtdEtn-diolein (10:85:5 mol%) was also examined (not shown). The polymorphic transition proceeds directly from the bilayer to the H_{II} without a significant isotropic phase. No significant changes in the composition of coexisting phases were observed.

TABLE 1 Polymorphism and phospholipid mixing in PtdCho/PtdEtn (1:3) with tetradecane

Tetradecane added wt%	Percentage bilayer	Percentage isotropic	Percentage inverted hexagonal	Percentage PtdCho in bilayer
0.0	100	0	0	25 ± 1.5
1.15	80	4	16	26.3 ± 1.5
1.3	45	1	54	26.0 ± 1.5
1.3*	41	2	57	26.1 ± 1.5
3.0	10#	0#	90#	—
10.0	0#	0#	100#	—

Data were obtained at 22°C and are based on phospholipid populations.
*Five hours after hydration (see text).
#Estimated from static spectra.

The fractional distribution of each phospholipid among the L_α, H_{II}, and I structures was plotted at several temperatures during the transition for the PtdMe-PamOlePtdEtn-diolein (20:75:5 mol%) mixture in Fig. 10. The PtdMe/PtdEtn ratios remained constant throughout the transition.

DISCUSSION

The equilibrium distribution of membrane constituents among lipid structures is strongly influenced by differences in packing and curvature. For example, the transbilayer distribution of membrane constituents in highly curved, sonicated vesicles is sensitive to packing factors. The inner and outer leaflets possess vastly different packing constraints and radii of curvature. Consequently, in sonicated lipid mixtures, the composition of each leaflet is generally different. Recent studies that examined the transbilayer distribution of phosphatidylethanol (PtdEt) in chain-homologous phosphatidylcholine vesicles demonstrated a fivefold preference of PtdEt for the inner leaflet (Victorov et al., 1994, 1997). The headgroup of PtdEt is much smaller than that of PtdCho. Because headgroup packing was much denser in the inner leaflet, the distributional preference of PtdEt for the inner leaflet was strongly expressed. This innate distributional preference for the inner leaflet was strongly countered at higher levels of anionic PtdEt by electrostatic factors that tended to equalize the transbilayer distribution. The resultant distribution was described quantitatively as a competition between packing and electrostatic factors.

Similar principles are expected to apply to polymorphism. Lipids, such as unsaturated PtdEtn, that possess a small headgroup and a large mean hydrocarbon volume (unsaturated chains or longer chains) tend to form inverted

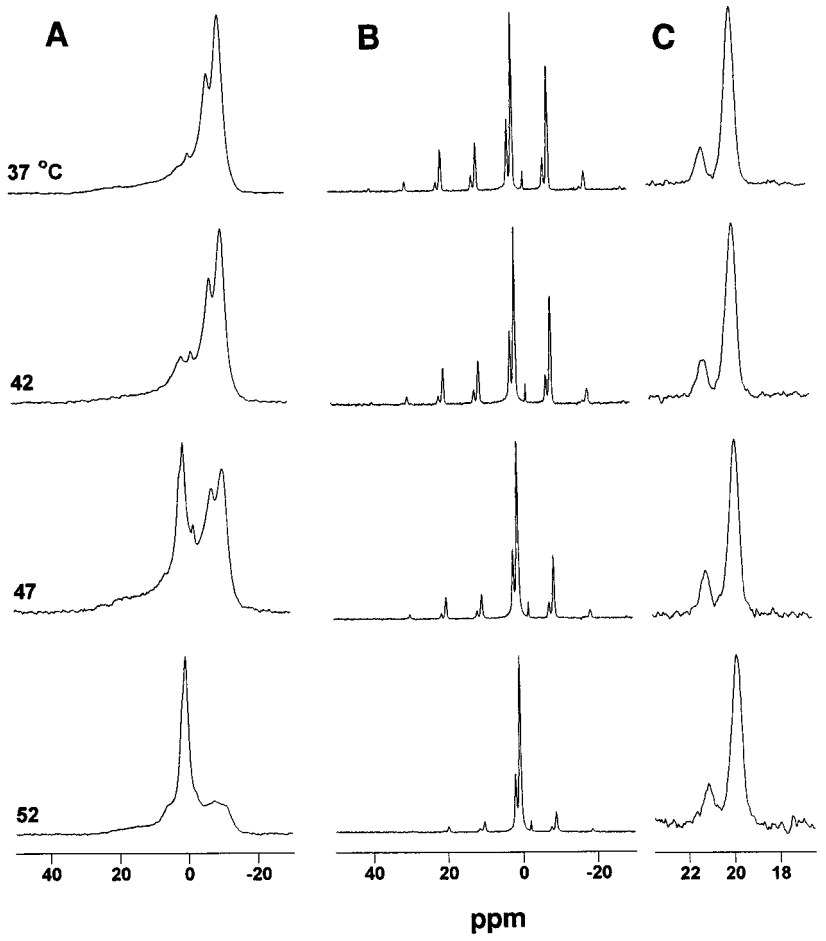

FIGURE 9 Distributional phase preferences of $Pam_2PtdMe/PamOlePtdEtn$/diolein at the temperatures indicated at (*A*) static and (*B*) MAS at 1400 Hz, and (*C*) expansion of second left sideband region of the spectra of *B*. The vertical expansions, in order from top to bottom, are 1, 1.15, 1.93, and 7.5.

phases in isolation and promote inverted phases in a mixture, and it would appear that they should exhibit a distributional preference for inverted phases in the phase coexistence regime of polymorphic transitions. The converse should apply to lipids, such as saturated PtdCho, that possess larger headgroups and smaller mean hydrocarbon areas (saturated chains or shorter chains). That such a simple picture was not operative in polymorphism was suggested by our observation that the ratio of the resolved asymmetries of ^{31}P bilayer powder patterns in binary lipid mixtures appeared constant in polymorphism (Lee et al., 1996).

Previous studies

Two studies have examined the composition of coexisting L_α and I structures, and both concluded that the structures had a similar composition. In each case the phospholipid resonances in the isotropic structure were resolved by high-resolution solution state ^{31}P NMR, and their intensities were found to be representative of the total sample composition. The systems investigated were egg PtdCho/cardiolipin/calcium (de Kruijff et al., 1979) and 1-palmitoyl-2-oleoyl PtdCho/dilinoleoyl PtdEtn (Boni and Hui, 1983).

In coexisting L_α and H_{II} structures, however, differing interpretations emerged. Tilcock et al. (1982) examined an $Ole_2PtdEtn/Ole_2PtdCho$ mixture (4:1) in the presence of varying amounts of cholesterol. Wideline ^2H NMR of either PtdCho or PtdEtn deuterated in the acyl chain region showed qualitatively similar spectra in the presence of coexisting L_α and H_{II} structures and indicated that the phospholipid composition was uniform for all phases throughout the $L_\alpha \rightarrow H_{II}$ transition. Other workers, however, found an enrichment of PtdCho in the L_α structure of PtdCho/PtdEtn mixtures under low water conditions, as determined by the deconvolution of the wideline ^{31}P powder patterns of the L_α structure. They suggested that the composition of coexisting L_α and H_{II} phases of mixtures was likely to differ (Eriksson et al., 1985). Subsequently, the system studied by Tilcock was reexamined by ^{31}P NMR studies of aligned mixtures. The approach yielded narrow resonances whose intensities confirmed the wideline ^2H NMR studies that indicated constant compositions (Fenske and Cullis, 1992). Yet x-ray diffraction studies of $Ole_2PtdCho/Ole_2PtdEtn$ mixtures in the presence of small amounts of tetradecane (td) were interpreted as showing up to a twofold enrichment of PtdCho for the bilayer structure (Rand et al., 1990). Other x-ray studies of $Ole_2PtdEtn$ containing a variety of unsaturated PtdCho in the absence of alkane were qualitatively supportive of this interpretation (Tate and Gruner, 1987). These results again cast doubt on the idea that the composition of

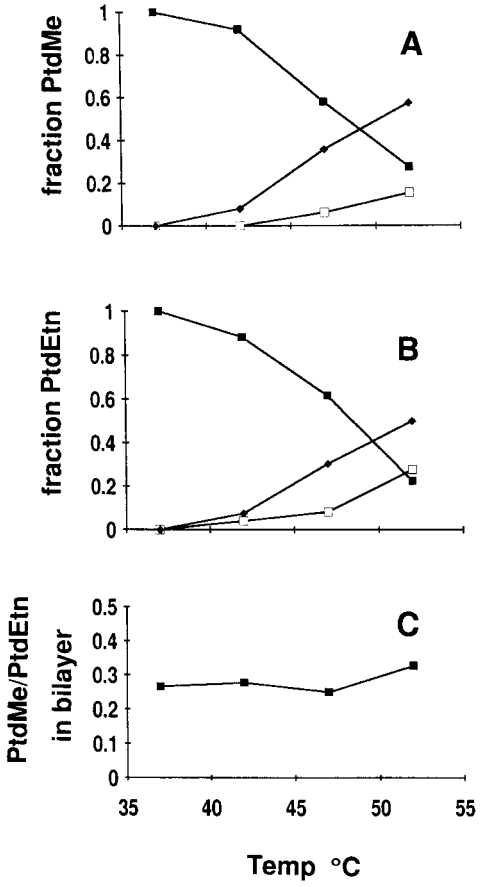

FIGURE 10 Distributional phase preferences in Pam_2PtdMe/PamOlePtdEtn/diolein (20:75:5). The fractions of (*A*) PtdMe and (*B*) PtdEtn in the bilayer (■), inverted hexagonal (□), and isotropic (♦) phases throughout the transition are shown. (*C*) The PtdMe/PtdEtn molar ratio in the bilayer.

coexisting phases was constant in polymorphism. In our work with phosphatidylalkanols in PtdEtn matrices using wideline ^{31}P NMR, we noted that the resolved perpendicular edge of the narrowed L_α phosphatidylalkanol tensor decreased in conjunction with the perpendicular edge of the broader L_α PtdEtn tensor and showed no evidence of marked distributional preferences in a PamOlePtdEtn matrix, but as with all wideline NMR studies cited, small changes in composition could have been overlooked (Lee et al., 1996).

A related situation occurs when the bilayer phospholipids are laterally segregated. In mixtures of gel-state bilayer-preferring and fluid-state H_{II}-preferring lipids, lateral sequestration of the gel-state L_α-preferring lipids allowed the fluid-state H_{II}-preferring lipids to undergo the $L_\alpha \rightarrow H_{II}$ transition (Tilcock and Cullis, 1982). The addition of calcium to lipid mixtures containing certain species of phosphatidylserine segregated the phosphatidylserine into crystalline domains and allowed the remaining lipids (PtdEtn) to undergo the $L_\alpha \rightarrow H_{II}$ transition (Tilcock and Cullis, 1981). In these cases the transition was incomplete, in contrast to the systems studied here. More germane to the present issue is whether nonidealities in lamellar lipid mixing, but not to the extent of lateral phase separation, are expressed in polymorphism as compositional heterogeneity, as discussed below.

Distribution of diunsaturated phospholipids

In agreement with the results reported by Tilcock et al. (1982) and Fenske and Cullis (1992) for fully hydrated Ole_2PtdCho/Ole_2PtdEtn/Chol mixtures, we found no quantitatively significant change in the phospholipid content of the phases throughout the $L_\alpha \rightarrow H_{II}$ transition. Although PtdCho prefers to adopt bilayer structures in isolation and stabilizes bilayer structures in PtdEtn mixtures, this preference was not expressed through its distribution between coexisting phases during the $L_\alpha \rightarrow H_{II}$ transition in this mixture.

A different situation, however, was previously reported for the same dioleoyl phospholipids in the presence of tetradecane and in the absence of cholesterol (Rand et al., 1990). PtdCho was thought to be enriched in the L_α structure, whereas PtdEtn was thought to be enriched in the H_{II}. This conclusion was reached indirectly by x-ray diffraction, and based on the observation that the first-order Bragg spacings of both coexisting L_α and H_{II} structures (i.e., their structural dimensions) were dependent on the amount of tetradecane added, and by assuming that the td-dependent changes in Bragg spacings could be correlated with changes in the PtdCho/PtdEtn composition ratios. In contrast, our direct measures of phospholipid populations indicate that the PtdCho/PtdEtn ratio is constant. The source of the discrepancy is unknown; however, in the current study the effects of td are larger than those observed in the diffraction study. The addition of 10 wt% td to our sample completely induced the H_{II} phase (Table 1), whereas the L_α phase was present in the diffraction study. Possibly our approach to td equilibration—incubation for 30 min with the dried lipid film—hastened equilibration and reduced td heterogeneity in the sample. These considerations are insufficient, however, to account for the changes in Bragg spacings reported in the phase coexistence region for unsaturated PtdCho, Ole_2PtdEtn mixtures in the absence of td (Tate and Gruner, 1987).

Distribution of anionic phosphatidylmethanol

Increases in the surface charge of membranes caused by the presence of anionic lipids induce electrostatic interactions in bilayers that strongly favor the maintenance of the bilayer structure vis à vis the H_{II} state (Epand and Bottega, 1988). It might be anticipated that these repulsive forces would be sufficient to induce a distributional preference of the anionic lipid for the bilayer and induce the depletion of the anionic lipid in the H_{II} state, where headgroup packing is tighter. Previously we examined anionic dioleoylphosphatidylethanol (10 mol%) in a 1-palmitoyl-2-oleoyl-phosphatidylethanolamine matrix by wideline ^{31}P NMR and found no

marked difference in the mixing properties of the phospholipids, based on comparisons of the distinct perpendicular edges of the respective powder patterns (Lee et al., 1996). Here we have used the MAS SSB technique to examine the distributional properties of dipalmitoylphosphatidylmethanol (10, 20 mol%) in a similar PamOlePtdEtn matrix (doped with 5 mol% diolein to lower the midpoint temperature). In neither case was the anionic lipid concentration enriched or depleted in any structure during polymorphism. Whereas the phosphatidylalkanols exhibit a number of unusual properties traced to the hydrophobic alkyl headgroup (Victorov et al., 1994; Lee et al., 1996), the electrostatics appear to be well behaved (Victorov et al., 1997). Thus electrostatic factors are not a strong promoter of compositional heterogeneity of coexisting structures in polymorphism.

Distribution of disaturated/diunsaturated phospholipids in the presence of cholesterol

In contrast to these results, significant changes in the composition of coexisting phases were observed in the Myr_2PtdCho/Ole_2PtdEtn/Chol and Lau_2PtdCho/Ole_2PtdEtn/Chol mixtures. In the absence of cholesterol, the composition of coexisting phases was constant in the Myr_2PtdCho/Ole_2PtdEtn system, suggesting that cholesterol was key to the expression of heterogeneity. Studies of the chain length dependence of polymorphism indicated that longer chain lengths generally promoted the formation of inverted structures, whereas shorter chain lengths promoted the formation of bilayer or normal micellar structures (Epand et al., 1989; Lewis and McElhaney, 1993; Seddon et al., 1983). From this standpoint, Lau_2PtdCho should have been more effective than Myr_2PtdCho in raising T_H and should have exhibited a more pronounced preference for the bilayer structure. The observed behavior was contrary to these expectations, with Myr_2PtdCho being more potent than Lau_2PtdCho in raising T_H and exhibiting a greater preference for the L_α structure. This indicated that the presence of cholesterol had modified the expected dependence of T_H on chain length.

The effects of cholesterol in polymorphism are complex. Cholesterol had a strong biphasic effect on the T_H of dielaidoyl (Ela_2) PtdEtn and similar but much weaker biphasic effects on PamOlePtdEtn and egg PtdEtn (Epand and Bottega, 1987). X-ray diffraction showed reflections characteristic of cholesterol domains ($>$ 35 mol%) in Ela_2PtdEtn and egg PtdEtn (Cheetham et al., 1989).

Other studies indicated that the miscibility of cholesterol strongly depended on the saturation of the phospholipid's acyl chains. Cholesterol (30 mol%) was shown to induce a fourfold decrease in the lateral diffusion of fluorescently labeled PtdEtn in saturated Myr_2PtdCho, but almost no change in diunsaturated Ole_2PtdCho (Kusumi et al., 1986). Subsequent studies (Pasenkiewicz-Gierula et al., 1990; Subczynski et al., 1990) showed that a variety of the actions of cholesterol were stronger on saturated PtdCho (and *trans*-diunsaturated PtdCho), but were greatly attenuated on *cis*-diunsaturated PtdCho. Together, these and other results were interpreted as indicative of low interaction enthalpies between cholesterol and the diunsaturated phospholipid chains due to packing mismatches between the rigid tetracyclic ring and the bend at the *cis* double bond. Nonideal mixing was postulated, with cholesterol-cholesterol and cholesterol-disaturate interactions being favored over cholesterol–*cis*-diunsaturate interactions (Subczynski et al., 1990; Pasenkiewicz-Gierula et al., 1990). Similar conclusions were reached by Shin and Freed (Shin and Freed, 1989a,b; Shin et al., 1990, 1993). These authors used orientational order parameters to estimate the thermodynamic activities of cholesterol and PtdCho. They also concluded that acyl chain unsaturation led to expulsion of Chol from the vicinity of the unsaturated phospholipid and thereby promoted the formation of cholesterol-rich microclusters.

Applying these interpretations to the Myr_2PtdCho/Ole_2PtdEtn/Chol (21:34:45) at hand, fluid-phase microimmiscibility in the bilayer was characterized by favored interactions between Myr_2PtdCho and Chol that, in turn, caused increased contacts among Ole_2PtdEtn molecules. Consequently, increased Ole_2PtdEtn contacts can be thought of as transient microclusters enriched in Ole_2PtdEtn that were more inclined to undergo the $L_\alpha \rightarrow H_{II}$ transition and, in turn, facilitate Ole_2PtdEtn enrichment in the H_{II} phase. Conversely, transient microclusters enriched in Myr_2PtdCho and Chol were less inclined to undergo the $L_\alpha \rightarrow H_{II}$ transition and allowed enrichment of Myr_2PtdCho and Chol in the bilayer. The smaller effects observed in the Lau_2PtdCho/Ole_2PtdEtn/Chol system could be ascribed to the short Lau chain length that was thought to be less able to accommodate Chol than longer acyl saturates (McIntosh, 1978), with its mixing behavior found to be intermediate between longer chain saturates and *cis*-diunsaturates (Kusumi et al., 1986). Here, no phospholipid enrichment was observed in the Ole_2PtdCho/Ole_2PtdEtn/Chol system. Because the acyl chains were homologous, Chol was unable to discriminate between PtdCho and PtdEtn on that basis and the PtdCho/PtdEtn ratio was constant, although the constancy of the Chol distribution was undetermined. Nor were differences in composition observed in the absence of cholesterol (Myr_2PtdCho/Ole_2PtdEtn, 1:4, or Ole_2PtdCho/Ole_2PtdEtn, 1:3). When the dimyristoyl chains of PtdCho were swapped with the dioleoyl chains of PtdEtn to form a quaternary mixture (Ole_2PtdCho/Myr_2PtdEtn/Ole_2PtdEtn/Chol, 21:21:13:45) with the same composite membrane shape as the Myr_2PtdCho/Ole_2PtdEtn/Chol (21:34:45) mixture, no significant change in the PtdCho/PtdEtn ratio was observed (although the PtdEtn resonance represented both Myr_2 and Ole_2 species). The transition was much narrower and the midpoint was elevated. This result is consistent with the scenario posed, in which Chol favored interactions with the saturated lipid—Myr_2PtdEtn after swapping—thereby replacing the increased contacts among Ole_2PtdEtn molecules (which strongly promote H_{II} structures) with increased contacts between Ole_2PtdCho and Ole_2PtdEtn (which is less inclined to promote H_{II} structures than Ole_2PtdEtn alone).

The nature of the lateral organization of cholesterol in the bilayer is beyond the scope of this article and is discussed at length in the cited articles. The main point here is that lateral microheterogeneities are likely to be expressed as compositional heterogeneity in the $L_\alpha \rightarrow H_{II}$ transition, with the distributional character based on the curvature propensity of the microclusters that are involved in the transition, rather than reflecting the distributional preferences of the individual membrane constituents.

Distributional preferences and transition width

A particularly striking and practical indication of the expression of compositional heterogeneity among coexisting phases was a broadening of the $L_\alpha \rightarrow H_{II}$ transition. The effect was quite dramatic, as observed for the Myr_2PtdCho/Ole_2PtdEtn/Chol system, where the transition width (75% $L_\alpha \rightarrow$ 25% L_α) was 28°C. With the composition of the bilayer changing continuously throughout the transition, the "midpoint" temperature for each composition also varied continuously, and an increase in the transition width occurred. Partition coefficients correlate linearly with composition over narrow ranges of the partition coefficient, such as those found here. Therefore, the linear correlation shown between the apparent partition coefficient and the transition width reflected the dependence of the transition width on the phospholipid composition.

Kinetically hindered or equilibrium distributions?

How is it that a lipid exhibits a strong preference for a particular phase in isolation, strongly stabilizes that phase in a mixture, and yet exhibits no distributional preference for that phase in the phase coexistence region of a thermotropic transition? Constraints imposed by the low aqueous solubility of phospholipid monomers eliminated the aqueous medium as a redistribution pathway, as would be applicable for a traditional partitioning mechanism. Compositional heterogeneity among phases was observed only when compositional heterogeneity preexisted within a phase. Our results were consistent with the concept that the lipid distribution among coexisting phases is governed by cooperative interactions where free diffusion of individual phospholipids among phases was hindered. The $L_\alpha \rightarrow H_{II}$ transition involves a macroscopic rearrangement of lipid morphology from vesicles to cylinders. This is quite distinct from the main transition, where coexisting structures are laterally juxtaposed and are in constant flux. Lipid exchange between coexisting L_α and H_{II} structures is very slow. No exchange of phospholipids between the L_α and H_{II} structures was detected over a period of at least several seconds (Fenske and Cullis, 1992). The kinetic barrier for structural interchange was further evidenced by the observation that increased contacts among lipid structures induced by increases in the lipid concentration or by sample pelleting significantly decreased the time required to attain equilibrium (Epand and Lemay, 1993). Consequently, there was little opportunity for statistical fluctuations in the composition of the cooperative assembly undergoing the transition, that would have enabled an individual constituent to establish its innate equilibrium distribution or partitioning behavior among structures.

This reasoning implies that the situation should be different for membrane constituents that possess an appreciable aqueous solubility that allows for the redistribution of individual molecules through a traditional partitioning mechanism (e.g., Janes et al., 1992). In those cases, individual molecules are not barred from expressing their innate distributional preferences. The likelihood of compositional heterogeneity should increase substantially. Furthermore, the aqueous reservoir, if very large, is capable of buffering changes in the agent's concentration as the transition progresses, and thereby can diminish the utility of the transition width as a marker for the presence of compositional heterogeneity.

The findings obtained here have relevance for the mechanism of the $L_\alpha \rightarrow H_{II}$ transition. That the preferred distributions are not expressed contraindicate transitional intermediaries that allow free diffusion of individual membrane constituents between coexisting L_α and H_{II} structures.

SUMMARY

A method of tracking phospholipid populations of coexisting phases in polymorphism was developed, based on the spinning sideband intensities of slow speed MAS ^{31}P NMR. Based on a selected sampling of lipid mixtures, the following hypotheses were drawn. The innate distributional preferences of individual phospholipids are not expressed during polymorphism. The composition of coexisting phases in polymorphism is homogeneous, unless nonideal mixing preexisting within a phase facilitates the formation of cooperative transitional lipid clusters that are compositionally heterogeneous. In such cases, the compositions of coexisting phases are likely to reflect the distributional preferences of the cluster ensemble. The formation of compositionally distinct phases during the $L_\alpha \rightarrow H_{II}$ transition is accompanied by an increase in the transition breadth. This increase should be regarded as a sign of possible compositional heterogeneity in cases where the compositions of coexisting phases are undetermined.

Supported by National Institutes of Health grants AA00163, AA07186, and AA07463, and a grant from the Alcoholic Beverage Medical Research Foundation.

REFERENCES

Boni, L. T., and S. W. Hui. 1983. Polymorphic phase behavior of dilinoleoylphosphatidylethanolamine and palmitoyloleoylphosphatidylcholine mixtures. Structural changes between hexagonal, cubic and bilayer phases. *Biochim. Biophys. Acta.* 731:177–185.

Cheetham, J. J., E. Wachtel, D. Bach, and R. M. Epand. 1989. Role of the stereochemistry of the hydroxyl group of cholesterol and the formation of nonbilayer structures in phosphatidylethanolamines. *Biochemistry*. 28:8928–8934.

de Bouregas, F. S., and J. S. Waugh. 1992. ANTIOPE, a program for computer experiments on spin dynamics. *J. Magn. Reson.* 96:280–289.

de Kruijff, B. 1997. Lipids beyond the bilayer. *Nature.* 386:129–130.

de Kruijff, B., P. R. Cullis, A. J. Verkleij, M. J. Hope, C. J. A. Van Echteld, and T. F. Taraschi. 1985. *In* The Enzymes of Biological Membranes, Vol. 1, 2nd Ed. A. N. Martonosi, editor. Plenum Press, New York. 131–204.

de Kruijff, B., A. J. Verkley, C. J. A. van Echteld, W. J. Gerritsen, C. Mombers, P. C. Noordam, and J. de Gier. 1979. The occurrence of lipidic particles in lipid bilayers as seen by ^{31}P NMR and freeze-fracture electron microscopy. *Biochim. Biophys. Acta.* 555:200–209.

Epand, R. M. 1985. Diacylglycerols, lysolecithin, or hydrocarbons markedly alter the bilayer to hexagonal phase transition temperature of phosphatidylethanolamines. *Biochemistry*. 24:7092–7095.

Epand, R. M. 1996. Functional roles of non-lamellar forming lipids. *Chem. Phys. Lipids.* 81:101–104.

Epand, R. M. 1997. Studies of membrane physical properties and their role in biological function. *Biochem. Soc. Trans.* 25:1073–1079.

Epand, R. M., and R. Bottega. 1987. Modulation of the phase transition behavior of phosphatidylethanolamine by cholesterol and oxysterols. *Biochemistry*. 26:1820–1825.

Epand, R. M., and R. Bottega. 1988. Determination of the phase behaviour of phosphatidylethanolamine admixed with other lipids and the effects of calcium chloride: implications for protein kinase C regulation. *Biochim. Biophys. Acta.* 944:144–154.

Epand, R. M., and C. T. Lemay. 1993. Lipid concentration affects the kinetic stability of dielaidoylphosphatidylethanolamine bilayers. *Chem. Phys. Lipids.* 66:181–187.

Epand, R. M., K. S. Robinson, M. E. Andrews, and R. F. Epand. 1989. Dependence of the bilayer to hexagonal phase transition on amphiphile chain length. *Biochemistry.* 28:9398–9402.

Eriksson, P.-O., L. Rilfors, G. Lindblom, and G. Arvidson. 1985. Multicomponent spectra from ^{31}P-NMR studies of the phase equilibria in the system dioleoylphosphatidylcholine-dioleoylphosphatidylethanolamine-water. *Chem. Phys. Lipids.* 37:357–371.

Fenske, D. B., and P. R. Cullis. 1992. Chemical exchange between lamellar and non-lamellar lipid phases. A one- and two-dimensional ^{31}P-NMR study. *Biochim. Biophys. Acta.* 1108:201–209.

Hornby, A. P., and P. R. Cullis. 1981. Influence of local and neutral anesthetics on the polymorphic phase preferences of egg yolk phosphatidylethanolamine. *Biochim. Biophys. Acta.* 647:285–292.

Hui, S.-W., and A. Sen. 1989. Effects of lipid packing on polymorphic phase behavior and membrane properties. *Proc. Natl. Acad. Sci. USA.* 86:5825–5829.

Israelachvili, J. N., S. Marcelja, and R. G. Horn. 1980. Physical principles of membrane organization. *Q. Rev. Biophys.* 13:121–200.

Janes, N. 1996. Curvature stress and polymorphism in membranes. *Chem. Phys. Lipids.* 81:133–150.

Janes, N., J. W. Hsu, E. Rubin, and T. F. Taraschi. 1992. Nature of alcohol and anesthetic action on cooperative membrane equilibria. *Biochemistry*. 31:9467–9472.

Kusumi, A., W. K. Subczynski, M. Pasenkiewicz-Gierula, J. S. Hyde, and H. Merkle. 1986. Spin-label studies on phosphatidylcholine-cholesterol membranes: effects of alkyl chain length and unsaturation in the fluid phase. *Biochim. Biophys. Acta.* 854:307–317.

Lee, Y.-C., T. F. Taraschi, and N. Janes. 1993. Support for the shape concept of lipid structure based on a headgroup volume approach. *Biophys. J.* 65:1429–1432.

Lee, Y.-C., Y. O. Zheng, T. F. Taraschi, and N. Janes. 1996. Hydrophobic alkyl headgroups strongly promote membrane curvature and violate the headgroup volume correlation due to "headgroup" insertion. *Biochemistry.* 35:3677–3684.

Lewis, R. N. A. H., and R. N. McElhaney. 1993. Calorimetric and spectroscopic studies of the polymorphic phase behavior of a homologous series of *n*-saturated 1,2-diacyl phosphatidylethanolamines. *Biophys. J.* 64:1081–1096.

McIntosh, T. J. 1978. The effect of cholesterol on the structure of phosphatidylcholine bilayers. *Biochim. Biophys. Acta.* 513:43–58.

Pasenkiewicz-Gierula, M., W. K. Subczynski, and A. Kusumi. 1990. Rotational diffusion of a steroid molecule in phosphatidylcholine-cholesterol membranes: fluid-phase microimmiscibility in unsaturated phosphatidylcholine-cholesterol membranes. *Biochemistry*. 29: 4059–4069.

Rand, R. P., N. L. Fuller, S. M. Gruner, and V. A. Parsegian. 1990. Membrane curvature, lipid segregation, and structural transitions for phospholipids under dual-solvent stress. *Biochemistry.* 29:76–87.

Seddon, J. M., G. Cevc, and D. Marsh. 1983. Calorimetric studies of the gel-fluid (L_β-L_α) and lamellar-inverted hexagonal (L_α-H_{II}) phase transitions in dialkyl- and diacylphosphatidylethanolamines. *Biochemistry*. 22:1280–1289.

Seelig, J., and A. Seelig. 1980. Lipid conformation in model membranes and biological membranes. *Q. Rev. Biophys.* 13:19–61.

Shin, Y.-K., and J. H. Freed. 1989a. Dynamic imaging of lateral diffusion by electron spin resonance and study of rotational dynamics in model membranes. Effect of cholesterol. *Biophys. J.* 55:537–550.

Shin, Y.-K., and J. H. Freed. 1989b. Thermodynamics of phosphatidylcholine-cholesterol mixed model membranes in the liquid crystalline state studied by the orientational order parameter. *Biophys. J.* 56:1093–1100.

Shin, Y.-K., D. E. Budil, and J. H. Freed. 1993. Thermodynamics and dynamics of phosphatidylcholine-cholesterol mixed model membranes in the liquid crystalline state: effects of water. *Biophys. J.* 65:1283–1294.

Shin, Y.-K., J. K. Moscicki, and J. H. Freed. 1990. Dynamics of phosphatidylcholine-cholesterol mixed model membranes in the liquid crystalline state. *Biophys. J.* 57:445–459.

Shyamsunder, E., S. M. Gruner, M. W. Tate, D. C. Turner, P. T. C. So, and C. P. S. Tilcock. 1988. Observation of inverted cubic phase in hydrated dioleoylphosphatidylethanolamine membranes. *Biochemistry*. 27: 2332–2336.

Subczynski, W. K., W. E. Antholine, J. S. Hyde, and A. Kusumi. 1990. Microimmiscibility and three-dimensional dynamic structures of phosphatidylcholine-cholesterol membranes: translational diffusion of a copper complex in the membrane. *Biochemistry.* 29:7936–7945.

Tate, M. W., and S. M. Gruner. 1987. Lipid polymorphism of mixtures of dioleoylphosphatidylethanolamine and saturated and monounsaturated phosphatidylcholines of various chain lengths. *Biochemistry*. 26: 231–236.

Tilcock, C. P. S., M. B. Bally, S. B. Farren, and P. R. Cullis. 1982. Influence of cholesterol on the structural preferences of dioleoylphosphatidylethanolamine-dioleoylphosphatidylcholine systems: a phosphorus-31 and deuterium nuclear magnetic resonance study. *Biochemistry.* 21:4596–4601.

Tilcock, C. P. S., and P. R. Cullis. 1981. The polymorphic phase behaviour of mixed phosphatidylserine-phosphatidylethanolamine model systems as detected by ^{31}P NMR. Effects of divalent cations and pH. *Biochim. Biophys. Acta.* 641:189–201.

Tilcock, C. P. S., and P. R. Cullis. 1982. The polymorphic phase behaviour and miscibility properties of synthetic phosphatidylethanolamines. *Biochim. Biophys. Acta.* 684:212–218.

Timken, H. K. C., N. Janes, G. L. Turner, S. L. Lambert, L. B. Welsh, and E. Oldfield. 1986. Solid-state oxygen-17 nuclear magnetic resonance spectroscopic studies of zeolites and related systems. *J. Am. Chem. Soc.* 108:7236–7241.

Victorov, A. V., N. Janes, G. Moehren, E. Rubin, T. F. Taraschi, and J. B. Hoek. 1994. Rapid transbilayer movement of phosphatidylethanol in unilamellar phosphatidylcholine vesicles. *J. Am. Chem. Soc.* 116: 4050–4052.

Victorov, A. V., N. Janes, T. F. Taraschi, and J. B. Hoek. 1997. Packing constraints and electrostatic surface potentials determine transmembrane asymmetry of phosphatidylethanol. *Biophys. J.* 72:2588–2598.

Woyciesjes, P. M., N. Janes, S. Ganapathy, Y. Hiyama, T. L. Brown, and E. Oldfield. 1985. Nitrogen and oxygen nuclear quadrupole and nuclear magnetic resonance spectroscopic study of N-O bonding in pyridine 1-oxides. *Magn. Reson. Chem.* 23:315–321.